NASA/TM—2018-219947 AIAA–2018–4499

NASA Low-Power Stirling Convertor for Small Landers, Probes, and Rovers Operating in Darkness

Scott D. Wilson, Nicholas A. Schifer, Steven M. Geng, and Terry V. Reid
Glenn Research Center, Cleveland, Ohio

Lawrence B. Penswick
Universities Space Research Association, Cleveland, Ohio

Michael R. Casciani
Vantage Partners, LLC, Brook Park, Ohio

November 2018

NASA STI Program . . . in Profile

Since its founding, NASA has been dedicated to the advancement of aeronautics and space science. The NASA Scientific and Technical Information (STI) Program plays a key part in helping NASA maintain this important role.

The NASA STI Program operates under the auspices of the Agency Chief Information Officer. It collects, organizes, provides for archiving, and disseminates NASA's STI. The NASA STI Program provides access to the NASA Technical Report Server—Registered (NTRS Reg) and NASA Technical Report Server—Public (NTRS) thus providing one of the largest collections of aeronautical and space science STI in the world. Results are published in both non-NASA channels and by NASA in the NASA STI Report Series, which includes the following report types:

- TECHNICAL PUBLICATION. Reports of completed research or a major significant phase of research that present the results of NASA programs and include extensive data or theoretical analysis. Includes compilations of significant scientific and technical data and information deemed to be of continuing reference value. NASA counter-part of peer-reviewed formal professional papers, but has less stringent limitations on manuscript length and extent of graphic presentations.

- TECHNICAL MEMORANDUM. Scientific and technical findings that are preliminary or of specialized interest, e.g., "quick-release" reports, working papers, and bibliographies that contain minimal annotation. Does not contain extensive analysis.

- CONTRACTOR REPORT. Scientific and technical findings by NASA-sponsored contractors and grantees.

- CONFERENCE PUBLICATION. Collected papers from scientific and technical conferences, symposia, seminars, or other meetings sponsored or co-sponsored by NASA.

- SPECIAL PUBLICATION. Scientific, technical, or historical information from NASA programs, projects, and missions, often concerned with subjects having substantial public interest.

- TECHNICAL TRANSLATION. English-language translations of foreign scientific and technical material pertinent to NASA's mission.

For more information about the NASA STI program, see the following:

- Access the NASA STI program home page at http://www.sti.nasa.gov

- E-mail your question to help@sti.nasa.gov

- Fax your question to the NASA STI Information Desk at 757-864-6500

- Telephone the NASA STI Information Desk at 757-864-9658

- Write to:
  NASA STI Program
  Mail Stop 148
  NASA Langley Research Center
  Hampton, VA 23681-2199

NASA/TM—2018-219947 AIAA–2018–4499

NASA Low-Power Stirling Convertor for Small Landers, Probes, and Rovers Operating in Darkness

Scott D. Wilson, Nicholas A. Schifer, Steven M. Geng, and Terry V. Reid
Glenn Research Center, Cleveland, Ohio

Lawrence B. Penswick
Universities Space Research Association, Cleveland, Ohio

Michael R. Casciani
Vantage Partners, LLC, Brook Park, Ohio

Prepared for the
International Energy Conversion Engineering Conference
sponsored by the American Institute of Aeronautics and Astronautics
Cincinnati, Ohio, July 9–11, 2018

National Aeronautics and
Space Administration

Glenn Research Center
Cleveland, Ohio 44135

November 2018

Acknowledgments

This work is funded through the NASA Science Mission Directorate and the Radioisotope Power Systems Program Office.
The authors wish to acknowledge Daniel Goodell, Paul Schmitz, Roy Tew, and Malcolm Robbie
for their contributions to the Mini Stirling development effort.

Level of Review: This material has been technically reviewed by technical management.

Available from

NASA STI Program
Mail Stop 148
NASA Langley Research Center
Hampton, VA 23681-2199

National Technical Information Service
5285 Port Royal Road
Springfield, VA 22161
703-605-6000

This report is available in electronic form at http://www.sti.nasa.gov/ and http://ntrs.nasa.gov/

NASA Low-Power Stirling Convertor for Small Landers, Probes, and Rovers Operating in Darkness

Scott D. Wilson, Nicholas A. Schifer, Steven M. Geng, and Terry V. Reid
National Aeronautics and Space Administration
Glenn Research Center
Cleveland, Ohio 44135

Lawrence B. Penswick
Universities Space Research Association
Cleveland, Ohio 44135

Michael R. Casciani
Vantage Partners, LLC
Brook Park, Ohio 44142

Summary

A variety of mission concepts have been studied by NASA and the U.S. Department of Energy (DOE) that would utilize low-power radioisotope power systems (RPS) for probes, landers, rovers, and repeaters. These missions would contain science instruments distributed across planetary surfaces or near objects of interest where solar flux is insufficient for using solar cells. Landers could be used to provide data like radiation, temperature, pressure, seismic activity, and other surface measurements for planetary science and to inform future mission planners. The studies proposed using fractional versions of the general purpose heat source (GPHS) or multiple lightweight radioisotope heater units (LWRHUs) to heat power conversion technologies for science instruments and communication. Dynamic power systems are capable of higher conversion efficiencies, which could enable equal power by using less fuel or more power by using equal fuel, when compared to less-efficient static power conversion technologies. Providing spacecraft with more power would decrease duty cycling of basic functions and, therefore, increase the quality and abundance of science data. Low-power Stirling convertors are being developed at NASA Glenn Research Center to provide future microspacecraft with electrical power by converting heat from one or more LWRHUs. An initial design converts multiple watts of heat to 1 W of electrical power output by using a Stirling convertor. Development of the concept includes the maturation of convertor and controller designs, performance evaluation of an evacuated metal foil insulation, and development of system interfaces. Demonstration of the convertor is planned and represents a new class of RPS with power levels an order of magnitude lower than previous practical designs.

Nomenclature

1D	one-dimensional
3D	three-dimensional
AC	alternating current
CAD	computer-aided design
CFD	computational fluid dynamics
DC	direct current
DOE	Department of Energy

GPHS	general purpose heat source
LWRHU	lightweight radioisotope heater unit
MLMI	multi-layer metal insulation
MOSFET	metal-oxide semiconductor field-effect transistor
PV	pressure-volume power
RHU	radioisotope heater unit
RPS	radioisotope power systems
TEC	thermoelectric couples
THD	total harmonic distortion

Symbols

CS_P	compression space volume adjacent to the power piston
CS_D	compression space volume adjacent to the displacer
ES_D	expansion space volume adjacent to the displacer
h_{cold}	enthalpy of gas at cold end of regenerator
h_{hot}	enthalpy of gas at hot end of regenerator
PV_{ESD}	pressure-volume power in the expansion space adjacent to the displacer
PV_{CSD}	pressure-volume power in the compression space adjacent to the displacer
PV_{PP}	pressure-volume power in the compression space adjacent to the power piston
PV	indicated or pressure-volume power
Q_{IN}	heat input
Q_{OUT}	heat output
T_a	acceptor temperature
T_r	rejector temperature
Δ	parasitic loss

1.0 Need for Low-Power Radioisotope Power Systems (RPS)

Low-power RPS conversion technologies that could convert very small amounts of heat to usable amounts of electric power include static thermoelectric couples (TEC) and dynamic Stirling convertors. Of the 51 missions studied by the Jet Propulsion Laboratory, Goddard Space Flight Center, and Ames Research Center, 27 of the missions used low-power systems that produced 5 mW to 9 W of electrical power (Ref. 1). The mission studies contained science instruments distributed across planetary surfaces or near objects of interest to measure data like wind, temperature, pressure, seismic activity, and other surface measurements for planetary science and to inform future mission planners. One such concept is shown in Figure 1. These studies used fractional versions of the general purpose heat source (GPHS) or one or more lightweight radioisotope heater units (LWRHUs) as a heat source. Energy storage, like batteries and supercapacitors, was required for most designs to enable periodic energy intensive functions like data collection, communications, and roving. These studies utilized thermoelectric technologies capable of 2- to 5-percent conversion efficiency, some of which had been demonstrated in a laboratory environment at that time. The study concluded that as the capability of each mission increased, so did the power requirements. There is a need for small RPS to power science monitoring stations and communication repeaters. Depending on the power requirements, small RPS could be used to enable a long-lived global monitoring network on the Moon to study geophysics and exospheric science (Ref. 2). Therefore, high-efficiency dynamic RPS could be used to increase science data return on future missions or become mission enabling for low-power applications.

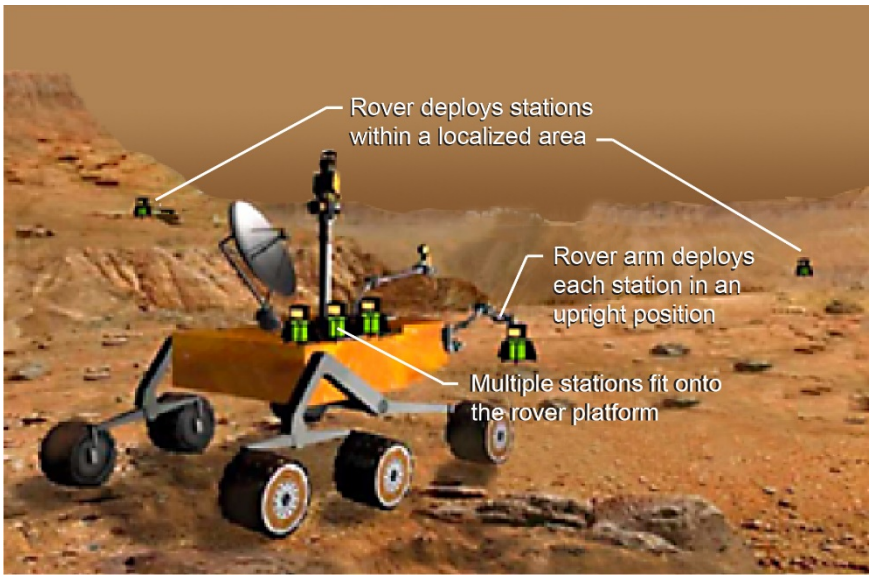

Figure 1.—Conceptualization of science monitoring stations being deployed from rover.

While NASA Glenn Research Center is developing 100-W-class power convertor designs for use with GPHS through contracted efforts, an in-house team was assembled to assess the feasibility of high-efficiency dynamic convertors at much lower power levels, suitable for use with LWRHUs. Initial efforts to develop subassemblies for a low-power dynamic RPS have led to a design that would convert heat from multiple LWRHUs to 1 W of usable direct current electric power for spacecraft instrumentation and communication (Ref. 3).

1.1 Heat Source

Early versions of the radioisotope heater unit (RHU) were developed for a lunar application and deep space exploration (Ref. 4). Following their successful use on the Pioneer and Voyager missions, a higher power density RHU was developed, called the LWRHU (Ref. 5). These smaller LWRHUs have a thermal output of 1.1 W at the beginning of life and have a 2.6 cm diameter and 3.2 cm length. Hundreds of LWRHUs have been used to provide localized heat on numerous spacecraft over the past few decades. These small heat sources have only been proposed as heat input for power applications but were never actually used. To enable convenient packaging and a similar cylindrical footprint to the Stirling convertor, two layers of four LWRHUs were selected for the initial concept. This concept would need to prevent helium created from the decay of the plutonium fuel from entering the evacuated insulation assembly over the life of the mission. Nuclear fuel is not available for laboratory testing, so electric resistance cartridge heaters are planned to enable demonstration and performance testing. The LWRHU electric simulator utilizes four vacuum-rated cartridge heaters to simulate the 8-W thermal input anticipated from the LWRHUs. Figure 2 shows the conceptual LWRHU heat source assembly with the LWRHU volumes (orange) and the cartridge heater volumes (red). The electrical wire bus will be powered by using a variable voltage power supply.

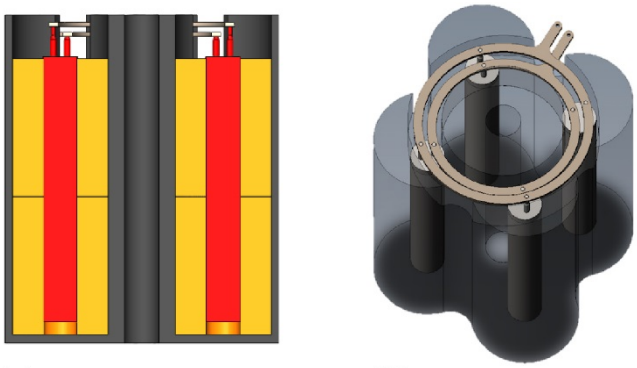

Figure 2.—Conceptual lightweight radioisotope heater unit (LWRHU) heat source assembly. (a) LWRHU volume shown in orange and cartridge heater volume shown in red. (b) Electrical wire bus.

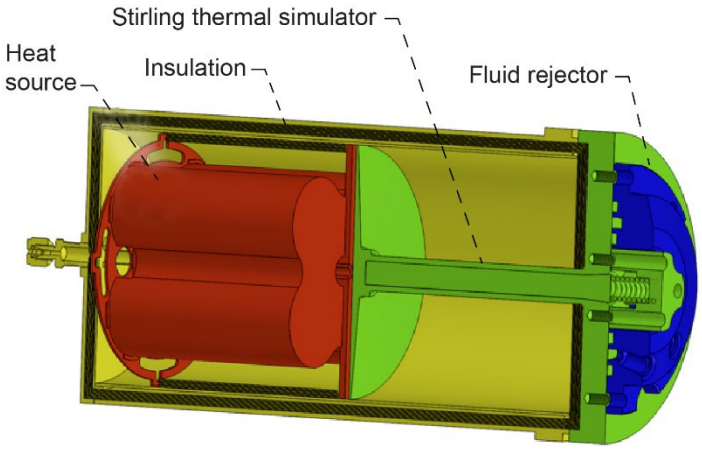

Figure 3.—Multi-layer metal insulation functional demonstration hardware, including electric heat source, Stirling thermal simulator, and fluid rejector.

2.0 Insulation

The heat flux coming from the surface of a LWRHU is about 274 W/m^2, while the heat flux from a GPHS is about 11,000 W/m^2. With so little heat available from the LWRHU, a highly effective insulation package is needed in order to achieve high efficiency and the desired hot-end temperatures for the Stirling convertor. To achieve that goal, a multi-layer metal insulation (MLMI) design is being provided by The Peregrine Falcon Corporation under contract with Glenn. The initial design utilizes metal foils to shield the heat that would be available from eight LWRHUs. Figure 3 shows a computer-aided design (CAD) image of the MLMI with the electric heat source, Stirling thermal simulator, and fluid heat rejector. The MLMI package utilizes strategically located thin metallic shields to minimize heat loss to the environment. The design is evacuated to eliminate convection heat transfer and minimize parasitic conduction losses at internal interfaces.

The Stirling thermal simulator is shown in Figure 3. The outer surfaces of the thermal simulator create a hermetic barrier between atmosphere and the evacuated insulation package. The thermal simulator is welded to a flange (not shown) to enable removal and inspection of the Stirling thermal

simulator. The insertion rod is instrumented with thermocouples to enable calculation of heat transfer through the assembly and validation of thermal models. The rod is external to the evacuated volume so it can be removed without disrupting the vacuum environment. A spring cup assembly is used to provide a light axial load to the rod, ensuring adequate contact during the test. A fluid heat exchanger is included to remove heat at the cold end of the assembly. This assembly should be adequate for testing in air or a vacuum.

3.0 Radioisotope Power Systems (RPS) (1 W)

The 1-W RPS are being developed to provide power options for microspacecraft or communication repeaters. Development efforts include maturation of the major subassemblies that make up the small RPS, consisting of a heat source assembly, Stirling convertor, electrical controller, and the insulation package and structure. The design effort has focused on the minimization of thermal and electrical losses for the insulation, convertor, and controller while providing a notional heat source assembly design. The heat source assembly would need further development to satisfy any safety requirements levied by the U.S. Department of Energy (DOE). The initial design currently contains a gas duct that connects the alternator to the engine but smaller configurations have been envisioned. Figure 4 shows an advanced concept that integrates the alternator and engine by using a mounting structure and internal gas passage, reducing the overall length. This RPS concept has an overall length of roughly 32 cm and a diameter of 11 cm. The heat source is mounted inside the insulation package and is radially constrained by using point contacts to minimize internal thermal losses. The heat source and Stirling hot end are radiatively coupled by using closely spaced plates. The Stirling convertor is constrained at the cold end and the heater head is radially constrained by using point contacts, similar to the heat source. This design would avoid mechanical loading of the Stirling heater head while still enabling an adequate Stirling hot-end temperature. The controller could be encapsulated in the housing and kept warm by the 4 W of waste heat available from the heat rejection flange located on the Stirling convertor. The current concepts have a total mass of under 3 kg.

Proof-of-concept hardware has been designed for easy assembly in a laboratory environment and is being prepared to support initial testing. A split-Stirling configuration was selected among a field of options and utilizes a gap regenerator and flexure bearings. The engine and alternator design parameters include a mean charge pressure of 7.5 bar and hot-end temperature of 350 °C, both of which are

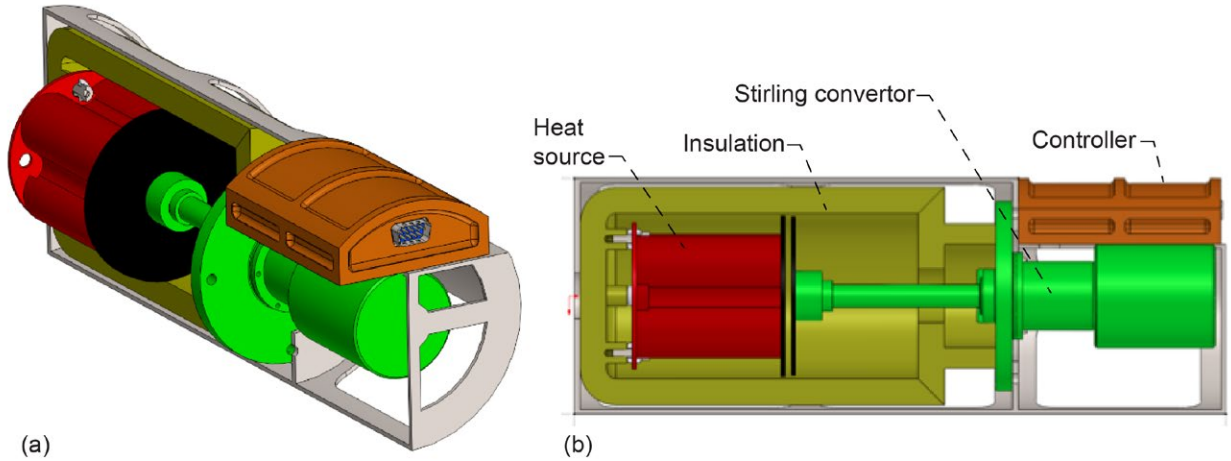

Figure 4.—Conceptual design for 1-W radioisotope power systems. (a) Angled, cutaway view. (b) Heat source, insulation, Stirling convertor, and controller.

considered to be relatively low compared to higher power designs for space (Table I). The hot-end temperature was selected in concert with anticipated insulation losses and an assumed value for maximum heat source surface temperature of 400 °C.

The Stirling cycle utilizes an operating frequency of 100 Hz and displacer and piston amplitudes of 2 and 4 mm, respectively. The initial design, shown in Figure 5, does not emphasize small size or low mass. The design was optimized for ease of inspection and parameter measurement, features that would not necessarily be present in flight designs. A thick-wall gas duct was used in place of a small-diameter gas line to enable testing of two different alternator designs, internal position sensors were included for displacer and piston position measurements, and a transducer was included for measurement of the compression-space dynamic pressure. Future versions will be used to address the minimization of sensors, interfaces, and containment vessel mass and/or size.

TABLE I.—STIRLING CONVERTOR (1 W) DESIGN PARAMETERS

Parameter	Target
Electrical output, W	1.3
Thermal input, Q_{IN}, W	6.8
Convertor efficiency, percent	20.0
Alternator efficiency, percent	90.0
Acceptor temperature, T_a, °C	350.0
Rejector temperature, T_r, °C	50.0
Frequency, Hz	100.0
Mean pressure, bar	7.6
Pressure amplitude, bar	0.9
Displacer amplitude, mm	2.0
Piston amplitude, mm	4.5

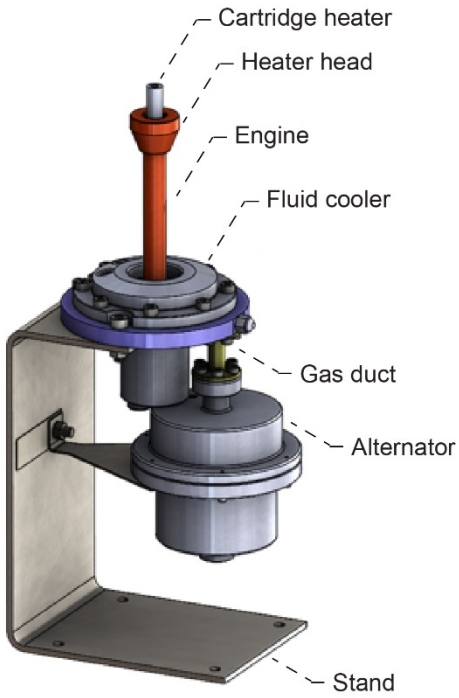

Figure 5.—Proof-of-concept design.
Insulation not shown.

3.1 Component Testing

The baseline alternator design for the 1-W Stirling convertor employs a moving coil and stationary iron and magnet. In this moving coil design, flexure bearings are used to conduct the induced current from the coil to the terminals inside the pressure vessel. This design utilizes a simple button magnet and iron construction, which has been optimized to reduce leakage of the magnetic flux fields. Figure 6 shows a cross section of the baseline alternator design.

As a potential alternative to the baseline, a new type of alternator was developed at Glenn by using a unique magnet layout and moving coil to convert linear shaft power into electricity (Ref. 6). Similar to the baseline, the moving coil is supported by flexure bearings, which also conduct the induced current from the coil to the terminals. A key feature of this new concept is the ultra-low inductance, which could eliminate the need for power factor correction and associated physical or digital tuning capacitors required by the controller to maximize the power factor. Initial fabrication has been completed and characterization testing of this low-inductance alternator has been initiated by using the test rig shown in Figure 7.

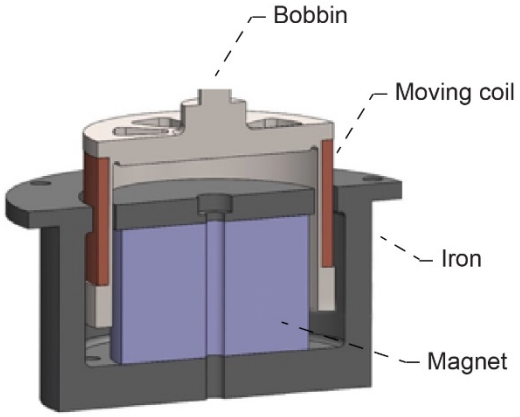

Figure 6.—Baseline moving coil design.

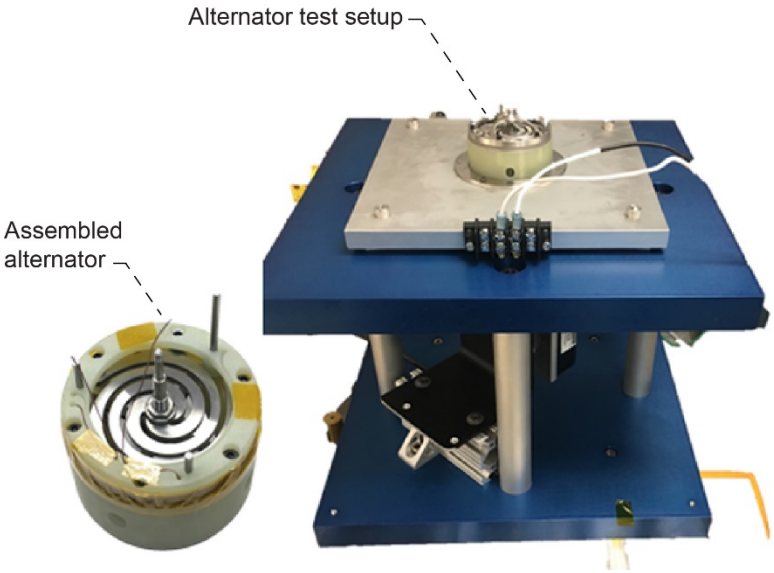

Figure 7.—Alternator characterization test rig.

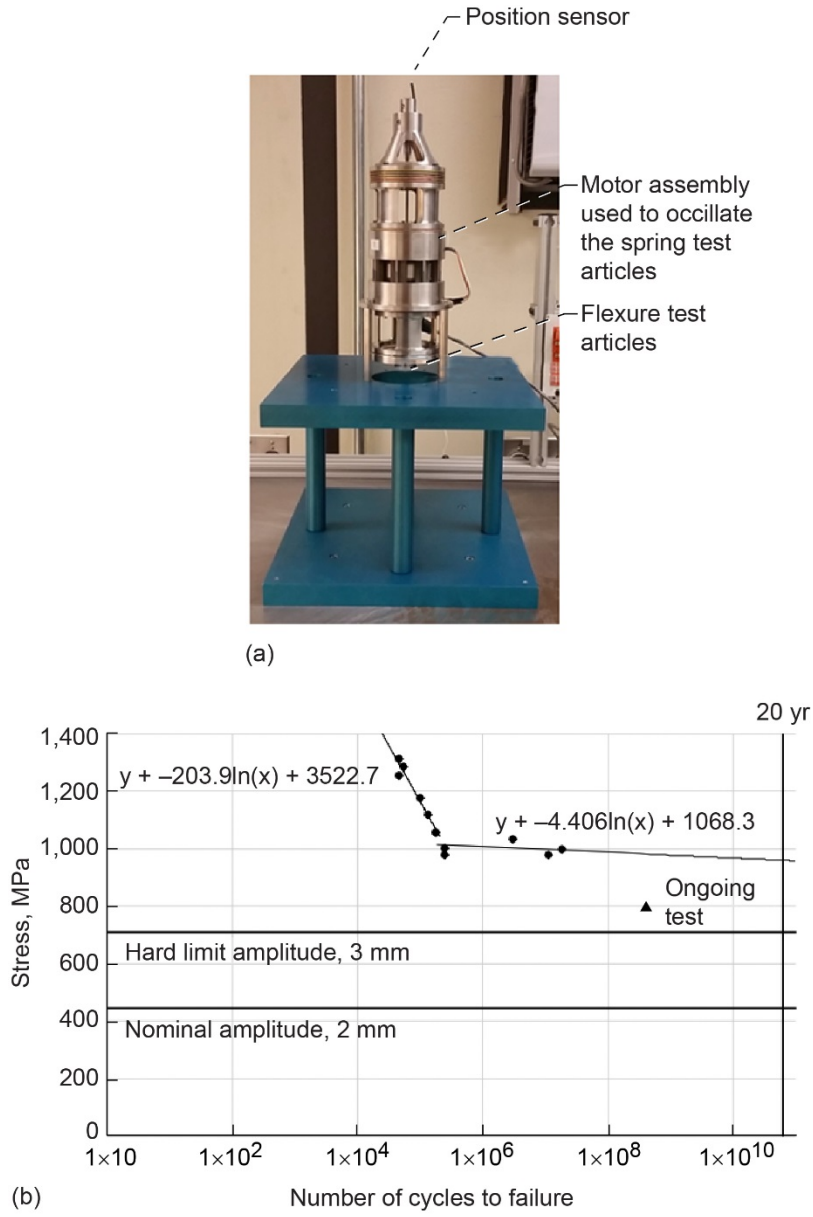

Figure 8.—Flexure test rig. (a) Flexure text rig and components. (b) Displacer flexure S-N curve test data from displacer flexure design (1095 spring steel).

A flexure test rig, shown in Figure 8, was also developed to enable fatigue testing of flexures at the design frequency through a range of amplitudes that exceed the design amplitude. The COMSOL Multiphysics® finite element modeling software (COMSOL Inc.) was used to model varying flexure designs and predict failure for a given deflection mode and value. Those displacer and piston flexures were then fabricated by using a chemical etching method. Subsequent testing of those designs was used to develop the stress versus number of cycles (S-N) curves, representing cyclic S-N to failure. However, the S-N curve could only be created for the displacer flexure because the motor amplitude was insufficient to fail any of the piston flexures. The displacer flexure test amplitudes varied from 3.4 to 5 mm, or 1.7 to 2.5 times higher than the nominal amplitude. These tests helped identify stress margins for desired design life of 20 yr. Flexures have been fabricated and tested for two different materials: 1095 carbon spring steel and Sandvik

7C27Mo2 (Sandvik AB). This first flexures were fabricated by using the 1095 carbon spring steel due to long lead times to receive the Sandvik material, the need to begin screening designs, and the need to develop prediction methods for design life. Through a literature search, the 1095 spring steel was found to have a better endurance fatigue limit on the order of 1,000 MPa compared to the Sandvik limit of 710 MPa; however, the Sandvik has the advantage of corrosion resistance, which is why it was selected. Both flexure designs were developed by using the material properties and stress limit for Sandvik. Figure 8 also shows the S-N curve developed for the 1095 spring steel displacer flexures, which shows plenty of stress margin between the maximum hard-stop amplitude of the device and the expected stress for failure based on test results. The stress was calculated for a given amplitude by using COMSOL Multiphysics® finite element analysis, and the number of cycles to failure was calculated from operating frequency and time. A sharp change in the slope of the S-N curve occurs at the empirical endurance limit, which matched well to the values found in the literature. Logarithmic trend lines were fit to the test data to project expected design life. An S-N curve has not yet been developed for displacer flexures of the Sandvik material; however, Sandvik flexures have been tested at 1.7 times nominal amplitude for 200 million cycles without failure. The piston flexure tests could only be performed at a maximum amplitude of 6 mm due to the limit of the drive motor current. That is still 1.2 times higher than the nominal amplitude and a value that exceeds the hard stop in the device. Both flexure designs were tested beyond 10 million cycles, a reasonable threshold for identifying the transition from high cycle fatigue to infinite life. The 1095 spring steel and Sandvik displacer flexures have been demonstrated up to 700 and 200 million cycles, respectively, at 1.7 times higher than the nominal amplitude without fracture. Similarly, the 1095 spring steel and Sandvik piston flexures have been demonstrated up to 500 and 100 million cycles, respectively, at 1.2 times higher than the nominal amplitude without fracture.

3.1.1 Controller

The Stirling convertor needs a controller that can maintain stability and rectify the power. An analog controller design is being developed at Glenn to control convertor dynamics and convert alternator alternating-current (AC) voltage to direct-current (DC) voltage for a spacecraft bus or energy storage system. The basic functionality provides load control, converts the AC to DC, provides waveform smoothing to improve total harmonic distortion (THD), and shunts excess electrical power when the energy storage is full. Initial designs of the analog controller were modeled in LTspice® (Analog Devices, Inc.) by using a linearized version of the alternator, a metal-oxide semiconductor field-effect transistor (MOSFET) H-bridge to rectify AC voltage to DC, a constant power circuit with a DC cap to smooth the voltage waveform and provide a DC voltage to the loads, and a synthetic capacitor to decrease THD and improve efficiency. Active filters were modeled to successfully lower the THD to acceptable levels: a THD of 4 percent, 75-percent controller efficiency, and over 1-We output. Breadboard testing is being performed to validate models and enable selection of an optimal design.

3.1.2 Advanced Modeling

The 1-W Stirling heat engine was modeled and optimized in Sage (Gedeon Associates), a commercially available thermodynamics code used to model heat engines and cryocoolers. The Sage code often contains computational errors on the order of 10 to 20 percent because it is a one-dimensional (1D) code and contains linearized relationships for some nonlinear physical phenomena. To gain confidence in the Sage results for this very low power machine, a computational fluid dynamics (CFD) model was created by using the commercially available Fluent code (ANSYS, Inc.). There are a few key differences between the 1D Sage model and the three-dimensional (3D) Fluent model. The Sage model connects fixed temperatures directly to the ends of the displacer cylinder, which artificially elevate the displacer

temperatures and associated axial parasitic heat transfer losses. The CFD model resolves those temperatures in an evolving thermal and fluid flow field. Additionally, the Sage model assumes no motion by the displacer when resolving heat transfer in that area, whereas the CFD model resolves temperature gradients and heat transfer by moving components and deforming gas volume meshes. The modeled domain was truncated at the piston face and displacer rod and, therefore, does not include seals or bounce spaces for either component.

Figure 9 shows the 3D computational domain. The Fluent calculations use two major boundary conditions, setting the acceptor cap volume to 625 K (352 °C) and the gas duct walls and rejector outer surface to 325 K (52 °C). The model used the steady solver until the temperatures propagated through the entire Fluent model. Once that was complete, the transient solver was activated and the motion characteristics of the displacer and piston were applied. This included mesh layering, which is applied to deforming meshes adjacent to any moving surfaces. Typically, 10 cycles were enough for the various parameters to become time periodic (where successive cycles of any parameters are identical). All output of interest is collected during the transient calculations at every time step and is used directly or postprocessed, if needed. Time histories of pressure and moving surfaces were used to build time histories of indicated or pressure-volume power (PV) for the power piston volume (CS_P), compression space adjacent the displacer (CS_D), and expansion space (ES_D). Once the results were confirmed to be time periodic, traces of all the relevant parameters were generated.

Table II shows the pressures and heat transfer averaged over the last cycle for Fluent as well as those predicted by Sage. Differences can be seen at the ends of the displacer cylinder in items 4 and 5. For Sage, the ends of the displacer cylinders have fixed hot- and cold-end temperatures applied to them, whereas Fluent resolves those temperatures. Without the extreme constant temperatures applied to the ends of the displacer cylinder in the Fluent model, the amount of heat entering the regenerator from the hot side is considerably higher when compared to the Sage model. This in turn limits the amount of heat in the Fluent model that is passed from the cylinders to the regenerator gas, which is shown as the enthalpy flux in Table II.

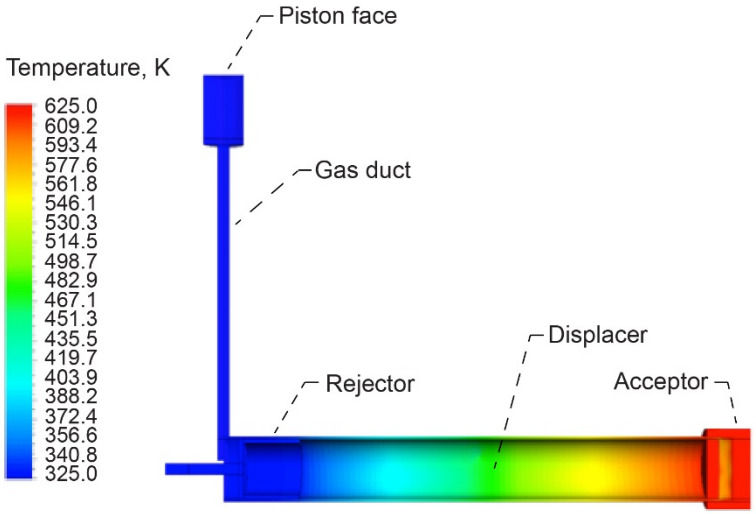

Figure 9.—Temperature contours across three-dimensional (3D) computational domain modeled in Fluent.

TABLE II.—HEAT DISTRIBUTION PREDICTIONS FOR ONE-DIMENSIONAL SAGE AND THREE-DIMENSIONAL FLUENT MODELS
[Baseline case: piston amplitude = 4.5 mm, displacer amplitude = 2 mm, and piston-displacer phase angle = 71°.]

Model type		Sage	Fluent
Pressure-volume power in the compression space adjacent to the displacer (PV_{CSD})		4.195	3.873
Pressure-volume power in the expansion space adjacent to the displacer (PV_{ESD})		4.195	3.992
Parasitic loss (Δ)		0.000	0.119
Shuttle heat transfer		.130	.115
Pressure-volume power in the compression space adjacent to the power piston (PV_{PP})		1.517	1.516
($PV_{ESD} - PV_{CSD} + PV_{PP}$)		1.517	1.635
Enthalpy of the gas at the hot end of the regenerator minus the enthalpy of the gas at the cold end of the regenerator ($h_{cold} - h_{hot}$)		.727	.143
Energy balances from the miniature Stirling model			
Model type		Sage	Fluent
Operating boundary condition		Fixed temperature surface	Fixed temperature volume
Heater acceptor temperature, K		625.0	625.0
Heater rejector temperature, K		325.0	325.0
Item	Description	Baseline	Baseline
1	Heat input (Q_{IN}) by acceptor	5.784	5.941
2	Expansion space	4.514	5.247
3	Enter hot heater head cylinder	.635	.694
4	Enter hot regenerator gas	.318	.926
5	Enter hot displacer cylinder	.635	.329
6	Exit cold heater head cylinder	.271	.589
7	Exit cold regenerator gas	1.046	1.069
8	Exit cold displacer cylinder	.271	.290
9	Rejection (Q_{OUT-1})	4.266	4.306
9a	Rejector	3.310	3.282
9b	Compression space adjacent the displacer (CS_D)	.781	.861
9c	Duct	.383	.316
9d	Displacer flex rod	.000	.040
9e	Piston face	.016	.439
10	Energy balance ($Q_{IN} - Q_{OUT}$)	1.518	1.635

Further, the Sage results do not directly account for shuttle heat transfer losses and show the indicated power PV_{CSD} and PV_{ESD} are equal. The Fluent model calculates these values to be slightly different, shown as parasitic loss in Table II. Shuttle loss is not directly calculated in Sage because the displacer is not moving in for the thermal calculations. Instead, a hand calculation was used to predict shuttle losses for the Sage results. In the Fluent model, shuttle loss is calculated by monitoring the net heat transfer

through the inner surfaces of the heater head and displacer cylinders adjacent to the regenerator while all of the relevant volumes are in motion.

The simulation effort resulted in similar values for the various features modeled between the two codes. While there were some differences, they are understood and there is confidence that both codes are indicating that this heat engine should perform well.

4.0 Conclusions

High-efficiency dynamic radioisotope power systems (RPS) could be used to increase science data return on future missions or could be mission enabling for low-power applications. NASA Glenn Research Center is developing a low-power dynamic RPS design that would convert heat from multiple lightweight radioisotope heater units (LWRHUs) to 1 W of usable direct-current electric power for spacecraft instrumentation and communication. The power system could be used to charge batteries or capacitors for higher power burst usage. A low-power free-piston Stirling convertor and controller are being fabricated by Glenn for initial demonstration and a facility test station with data systems has been prepared. Development also includes the maturation of a highly efficient multi-layer metal insulation (MLMI) package. Proof-of-concept hardware is being prepared to demonstrate this new class of power conversion device in a laboratory environment. This power system could be matured for small probes, landers, rovers, and communication repeaters needed on future space exploration missions.

References

1. Abelson, Robert D., et al.: Enabling Exploration With Small Radioisotope Power Systems. JPL Pub 04–10, 2004.
2. Jawin, Erica R., et al.: Lunar Science for Landed Missions Workshop Findings Report. Presented at the Lunar Science for Landed Missions Workshop, Moffett Field, CA, 2018.
3. Wilson, Scott D., et al.: Radioisotope Heater Unit-Based Stirling Power Convertor Development at NASA Glenn Research Center. NASA/TM—2018-219704 (AIAA 2017–4715), 2018. http://ntrs.nasa.gov
4. National Aeronautics and Space Administration: Environmental Statement for Mariner Jupiter/Saturn Project. NASA–741756–D, 1973.
5. Tate, R.E.: The Light Weight Radioisotope Heater Unit (LWRHU): A Technical Description of the Reference Design. LA–9078–MS, 1982.
6. Geng, Steven M.; and Schifer, Nicholas A.: Development of a Low Inductance Linear Alternator for Stirling Power Convertors. AIAA 2017–4961, 2017.